Nonlinear Dynamics **11:** 83–106, 1996.

Deterministic and Stochastic Analyses of Chaotic and Overturning Responses of a Slender Rocking Object

H. LIN and S. C. S. YIM
Ocean Engineering Program, Department of Civil Engineering, Oregon State University, Corvallis, OR 97331-2302, U.S.A.

(Received: 7 January 1994; accepted: 14 November 1995)

Abstract. The relationship between chaos and overturning in the rocking response of a rigid object under periodic excitation is examined from both deterministic and stochastic points of view. A stochastic extension of the deterministic Melnikov function (employed to provide a lower bound for the possible chaotic domain in parameter space) is derived by taking into account the presence of random noise. The associated Fokker–Planck equation is derived to obtain the joint probability density functions in state space. It is shown that global behavior of the rocking motion can be effectively studied via the evolution of the joint probability density function. A mean Poincaré mapping technique is developed to average out noise effects on the chaotic response to reconstruct the embedded strange attractor on the Poincaré section. The close relationship between chaos and overturning is demonstrated by examining the structure of the invariant manifolds. It is found that the presence of noise enlarges the boundary of possible chaotic domains in parameter space and bridges the domains of attraction of coexisting responses. Numerical results consistent with the Foguel alternative theorem, which discerns asymptotic stabilities of responses, indicate that the overturning attracting domain is of the greatest strength. The presence of an embedded strange attractor (reconstructed using the mean Poincaré mapping technique) indicates the existence of transient chaotic rocking response.

Key words: Slender rocking object, chaotic, overturning, deterministic, stochastic, invariant manifolds, generalized stochastic Melnikov process, Fokker–Planck equation, probability density function (PDF), Foguel alternative theorem, mean Poincaré map.

1. Introduction

An in-depth understanding of the rocking behavior of rigid block-like structures is essential to mechanical and civil engineers in the design and maintenance of a variety of free-standing structures such as petroleum storage tanks, water towers, nuclear reactors, concrete radiation shields and equipment racks subjected to base excitations due to earthquake ground motions, and/or nearby machine vibrations [1–8]. It is well-known that the rocking response is highly nonlinear and can be very sensitive to small variations in system parameters and excitation details [1, 2]. Probabilistic trends can only be established with a large sample size [2]. Koh [9] studied rocking response subjected purely random excitations through simulation and estimated the probability of no toppling. For simplicity of analysis and demonstration purpose, random excitations are usually assumed to be stationary delta-correlated (i.e. white) noise. Iyengar and Manohar [10] investigated the stochastic rocking behavior under simultaneous horizontal and vertical white-noise excitations. By approximating the impact-induced energy dissipation by viscous damping and assuming no overturning under weak noise perturbations, an approximate stationary solution of the probability density function (PDF) was obtained. Another probabilistic analysis on the stochastic rocking response was carried out by Dimentberg et al. [11]. The base excitations were modelled as white noise in both horizontal and vertical directions, and both free-standing and anchored objects were considered. They found

that, similar to the statistical results obtained by Yim et al. [2], larger blocks are more stable than smaller ones of the same geometric proportion.

Recognizing the insurmountable difficulties in the analysis of the complex behavior of the fully nonlinear rocking objects subjected to quake excitations, Spanos and Koh [3] simplified the SDOF model by assuming the rigid objects to be slender and the base excitation to be harmonic. They were able to develop approximate analytical methods to predict the existence and stability of harmonic and subharmonic responses. A significant understanding about the nonlinear behavior of the rocking object was gained through such a study. However, as pointed out by Wong and Tso [4] in their experimental study of the simplified system, there appear to be responses that could not be accounted for by the classical analytical methods.

These unpredicted responses were further investigated and later identified to be chaotic [5, 6]. Hogan [5] developed a discrete mapping technique to determine the stability regions of harmonic and subharmonic responses and identified the regions of possible chaotic response. He also quantitatively matched his analytical predictions with Wong and Tso's experimental results. Yim and Lin [6–8] examined the response behavior of both slender and non-slender rocking objects subjected to simple deterministic excitations. They found that, although chaotic time histories have a periodic time-dependency (thus non-stationary), time series consisting of Poincaré points of chaotic responses possess stochastic invariant properties which indicate a strong link between deterministic and stochastic behaviors.

This paper extends the deterministic studies of Yim and Lin [6–8] and investigates the chaotic and overturning responses of a free-standing rigid object subjected to horizonal periodic excitation under the influence of random noise. As indicated in [12], effects of slenderness of the block on the chaotic rocking response are not significant in the Melnikov sense. Thus, the rigid object is considered "slender" here as in [6] and [8] for simplicity and to isolate the nonlinear effects due to impact. The effects of system parameters including slenderness ratio, spectral characteristics of noise and non-stationarity of the excitation to the rocking responses is being investigated and documented [13].

For the rocking block in a deterministic state (without noise perturbations), the Melnikov function will be employed to provide a criterion for the existence of chaotic response. Invariant manifolds will be constructed to reflect a close relationship between chaotic and overturning responses and to identify the imprint of the safe region for bounded rocking responses (chaos). For the rocking block in a stochastic state, a generalized stochastic version of the Melnikov criterion will be derived by taking into account the presence of noise. The corresponding Fokker–Planck equation will be derived and solved for the PDF using a path integral solution procedure. Global information of the rocking behavior will be demonstrated via the evolution of the PDF. By applying a mean Poincaré mapping technique [14], noise-induced random perturbations of the chaotic responses are averaged out and the embedded strange attractor can be reconstructed on the Poincaré section. The presence of the reconstructed chaotic attractor indicates the possible existence of transient chaotic rocking response. The capability and limitations of this mapping technique will be also examined in detail. The numerical results are then interpreted in light of the Foguel alternative theorem which asserts the conditions for the existence of invariant measures and signifies asymptotic stabilities of system responses.

2. System Considered

As described in [2] and [6], a free-standing slender object is modelled as a rectangular rigid body subjected to horizontal base motion excitation (Figure 1). Assuming that friction at the

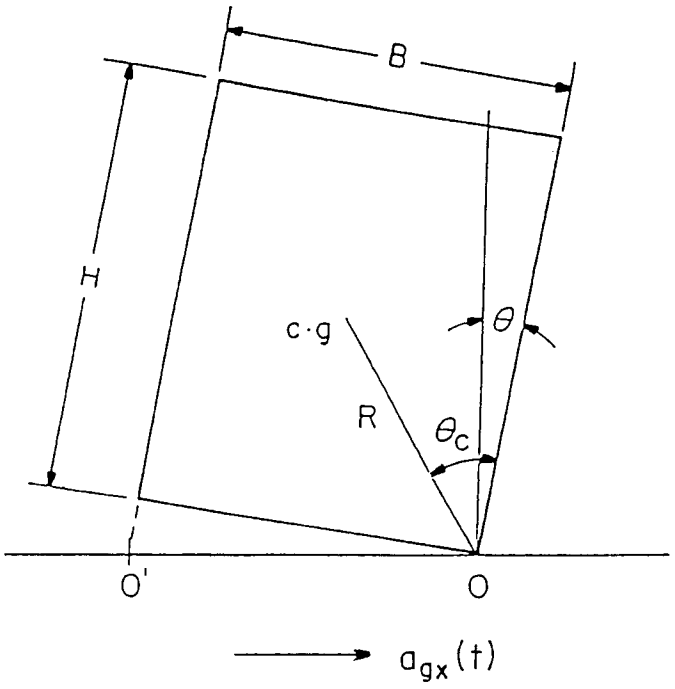

Figure 1. Idealization of free-standing equipment as rigid rocking objected to horizontal excitation.

interface between the rigid object and the base is sufficiently large so that there is no slipping, depending on the support accelerations, the body may move rigidly with the base or be set into rocking motion. If rocking occurs, it is assumed that the body will oscillate rigidly about the centers of rotation O and O'. The governing equation of motion about corner O (O') with positive (negative) angle of the rocking response is given by equation (1a) (equation (1b)):

$$I_0\ddot{\theta} + MRa_{gx} + MgR(\theta_{cr} - \theta) = 0, \qquad \theta > 0 \tag{1a}$$

and

$$I_0\ddot{\theta} + MRa_{gx} - MgR(\theta_{cr} + \theta) = 0, \qquad \theta < 0, \tag{1b}$$

where I_0 = moment of inertia about O or O'; M = mass; a_{gx} = the horizontal base acceleration; R = the distance from O to the center of mass; and $\theta_{cr} = \cot^{-1}(H/B)$ = the critical (static overturning) angle, where H and B = the height and width of the object. Impact occurs when the angular rotation crosses zero approaching from the positive (negative) direction and the base surfaces re-contact. Impact-induced energy loss (or damping) is accounted for by a coefficient of restitution, e, which relates the angular velocities before and after impact [2]

$$\dot{\theta}(t^+) = e\dot{\theta}(t^-) \qquad 0 \leq e \leq 1, \tag{2}$$

where t^+ (t^-) = the time just after (before) impact. In this study, a deterministic horizontal based motion excitation is considered sinusoidal, and any uncertainties/imperfections to the sinusoidal excitation are deemed random perturbations which are approximated by an additive white noise [15]. The white noise model provides an appropriate approximation when the noise

correlation time is much shorter than the system relaxation time, which is generally true for rocking systems. The horizontal base excitation is then given by

$$a_{gx}(t) = a\cos(\omega t + \phi) + \xi(t), \tag{3}$$

where a, ω and ϕ are the amplitude, frequency and phase shift of the periodic excitation, respectively. ξ describes a zero-mean, delta-correlated white noise perturbations with intensity q. In the limit as $q \to 0$, the system becomes deterministic as the excitation approaches purely periodic. As a first step towards understanding the influence of random noise on chaotic response, only idealized stationary Gaussian white noise is used in this study for simplicity of analysis and interpretation. (Numerical results indicate that white and non-white noises have similar effects on rocking response when their energy levels are equivalent [16].) Effects due to noise non-stationarity and spectral characteristics, which require extensive numerical simulations, is examined in a separate study [13].

For convenience of analysis, non-dimensionalized versions of equations (1a) and (1b) are employed. Dividing both equations by the moment of inertia and the critical angle, and re-scaling time [6], equations (1a) and (1b) become

$$\ddot{\Theta} - \Theta = -A\cos(\Omega\tau + \Phi) + \eta(\tau) - 1, \qquad \Theta > 0 \tag{4a}$$

and

$$\ddot{\Theta} - \Theta = -A\cos(\Omega\tau + \Phi) + \eta(\tau) + 1, \qquad \Theta < 0, \tag{4b}$$

where Θ = non-dimensionalized angle; A, Ω and Φ = non-dimensionalized amplitude, frequency and phase shift of the periodic excitation. η is the re-scaled zero-mean delta-correlated white noise with re-scaled intensity k;

$$E[\eta(\tau)] = 0$$
$$E[\eta(\tau)\eta(\tau')] = \kappa(\tau - \tau'). \tag{5}$$

Thus, the system response is governed by two linear stochastic differential equations with a local velocity discontinuity at zero displacement (i.e., impact, characterized by e). This discontinuity causes the rocking response behavior to be highly nonlinear [5–8]. The system behavior is analyzed in state space by setting state variables

$$x_1 = \Theta, \qquad x_2 = \dot{\Theta}. \tag{6}$$

The corresponding phase portrait with three fixed points, $(+1, 0)$, $(-1, 0)$ and $(0, 0)$, is shown in Figure 2. Two heteroclinic orbits are represented by the solid lines, and dashed lines represent sample phase trajectories with different initial conditions.

By including external excitation and energy dissipation as perturbations, the governing equation for the rocking system can be expressed in vector form:

$$\dot{X} = f_{1,2}(X) + g(X, \tau) \tag{7a}$$

with

$$X = \begin{Bmatrix} x_1 \\ x_2 \end{Bmatrix}, \qquad f_1(X) = \begin{Bmatrix} x_2 \\ x_1 - 1 \end{Bmatrix}, \qquad f_2(X) = \begin{Bmatrix} x_2 \\ x_1 + 1 \end{Bmatrix} \tag{7b}$$

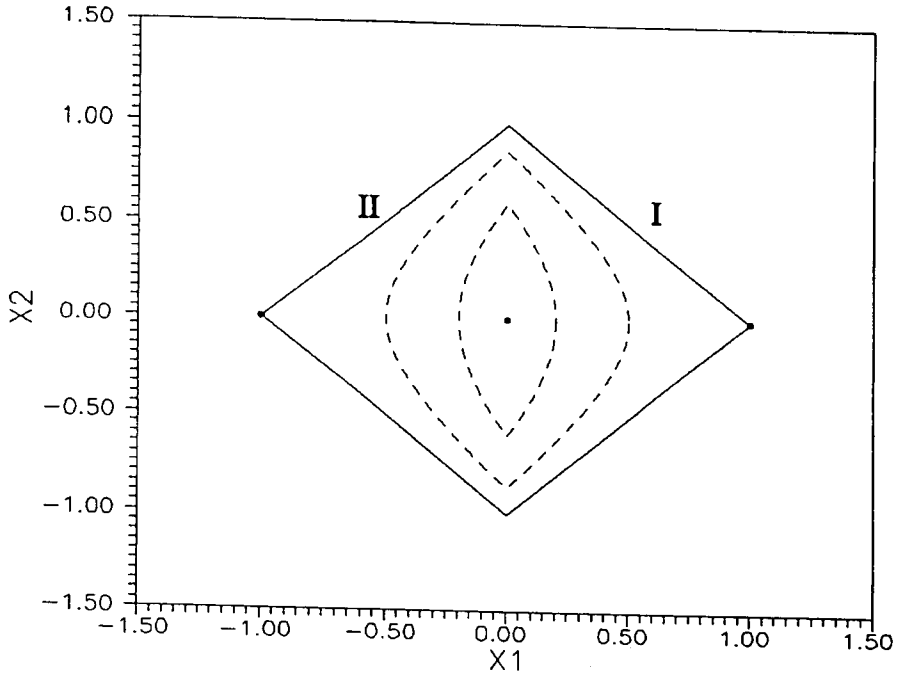

Figure 2. Phase portray of the unperturbed (Hamiltonian, $e = 1.0$) rocking system.

and

$$g(X,\tau) = \left\{ \begin{array}{c} 0 \\ -A\cos(\Omega\tau + \Phi) - \frac{1}{2}\, x_2^2(1-e^2)\delta(x_1) + \eta(\tau) \end{array} \right\} \tag{7c}$$

in which the energy dissipation due to impact is represented by the Dirac delta function [6].

3. Methods of Analysis

3.1. Deterministic State

When a rigid block is under purely periodic excitation, the system is said to respond in a deterministic state. The associated Melnikov function has been developed by Yim and Lin [6] to identify possible existence of chaotic response. Invariant manifolds will be constructed in this section to indicate the basin of attraction for bounded rocking response (safe region) on the Poincaré section.

3.1.1. *Melnikov Method*

The Melnikov method provides a quantitative representation of the existence of the transverse intersection of homoclinic orbits and hyperbolic periodic orbits, thus identifying possible chaotic response, in a two dimensional vector field [17, 18]. For convenience of reference, and later comparison with stochastic extensions, the deterministic results obtained by Yim and Lin [6] are briefly summarized here.

The heteroclinic orbits in regions I and II (Figure 2) can be expressed by explicit time functions [6]

$$q_{\mathrm{I}}^0(\tau) = (1 - e^{-\tau}, e^{-\tau}), \qquad q_{\mathrm{II}}^0(\tau) = (e^{\tau} - 1, e^{\tau}). \tag{8}$$

Because of symmetry of the heteroclinic orbits with respect to x_1, in the phase plane, only the upper heteroclinic orbit needs to be examined. Assuming perturbations, $x_2^2(1 - e^2)\delta(x_1)/2$, $A\cos\Omega\tau$ and $\eta(\tau)$, small, the Melnikov function is given by

$$\begin{aligned} M_d^+(\tau_{10}) &= \int_{-\infty}^{\infty} f[q_{\mathrm{I,II}}^0(\tau)] \bigwedge g[q_{\mathrm{I,II}}^0(\tau); \tau_{10}]\, \mathrm{d}\tau \\ &= \int_{-\infty}^{0} f[q_{\mathrm{II}}^0(\tau)] \bigwedge g[q_{\mathrm{II}}^0(\tau); \tau_{10}]\, \mathrm{d}\tau + \int_{0}^{\infty} f[q_{\mathrm{I}}^0(\tau)] \bigwedge g[q_{\mathrm{I}}^0(\tau); \tau_{10}]\, \mathrm{d}\tau \\ &= -\frac{2A\cos(\Omega\tau_{10})}{1 + \Omega^2} - \frac{1}{2}(1 - e^2), \end{aligned} \tag{9}$$

where the superscript "+" signifies the upper heteroclinic orbit. $M_d^+(\tau_{10})$ represents the Melnikov function due to the deterministic perturbations, i.e., periodic excitation and impact. The Melnikov function will equal zero for some τ_{10} when the following condition is satisfied

$$\frac{1 - e^2}{2} = -\frac{2A\cos(\Omega\tau_{10})}{1 + \Omega^2}\,. \tag{10}$$

The criterion for possible chaos in the rocking system is then given by

$$\frac{1 - e^2}{2} \leq \frac{2A}{1 + \Omega^2}\,. \tag{11}$$

The lower bound based on the Melnikov criterion in the A–Ω domain is shown by the solid line in Figure 3. Deterministic chaotic rocking response may occur when the excitation parameters (A and Ω) fall in the region above the lower bound.

3.1.2. *Invariant Manifolds*

As mentioned in the Melnikov analysis, chaotic response may occur when the stable and unstable manifolds intersect each other transversely. The invariant structures of the stable and unstable manifolds can be obtained on the Poincaré section through a mapping technique [19] and numerical simulations [20].

The saddles and center, which are located at $(\pm 1, 0)$ and $(0, 0)$ in the Hamiltonian system (Figure 2), are shifted due to the presence of perturbations (periodic excitation). The direction and magnitude of the shifts are closely related to the amplitude and frequency of the excitation [19]. It is noted that there is no conventional (continuous) damping mechanism in the rocking system, and impact-induced energy loss occurs locally at zero angular displacement during re-contact. Thus, impact may influence the structure of the invariant manifolds but does not shift the saddle points. Through local linearizations, the eigenvectors corresponding to each shifted saddle can be obtained (Hartman–Grobman theorem, [17]).

Along the principal (eigen) direction of the saddle on the left, a selected small segment of the eigenvector is divided into a finite number of infinitesimal elements which are individually

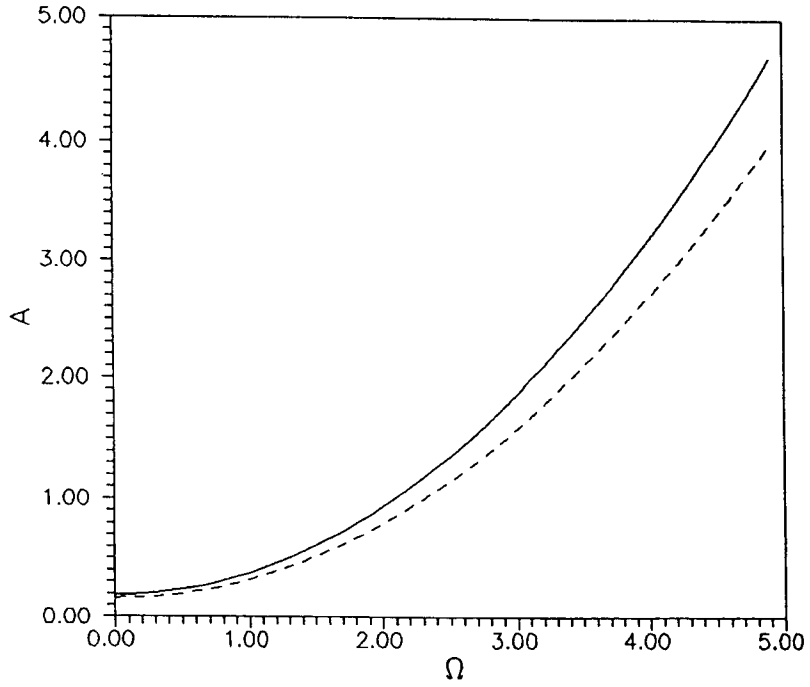

Figure 3. Stochastic/deterministic Melnikov criteria for chaotic rocking response (lower bound in A–Ω domain): solid and dashed lines represent the cases without ($\kappa = 0.0$) and with noise disturbance ($\kappa = 0.001$), respectively; with $e = 0.5$.

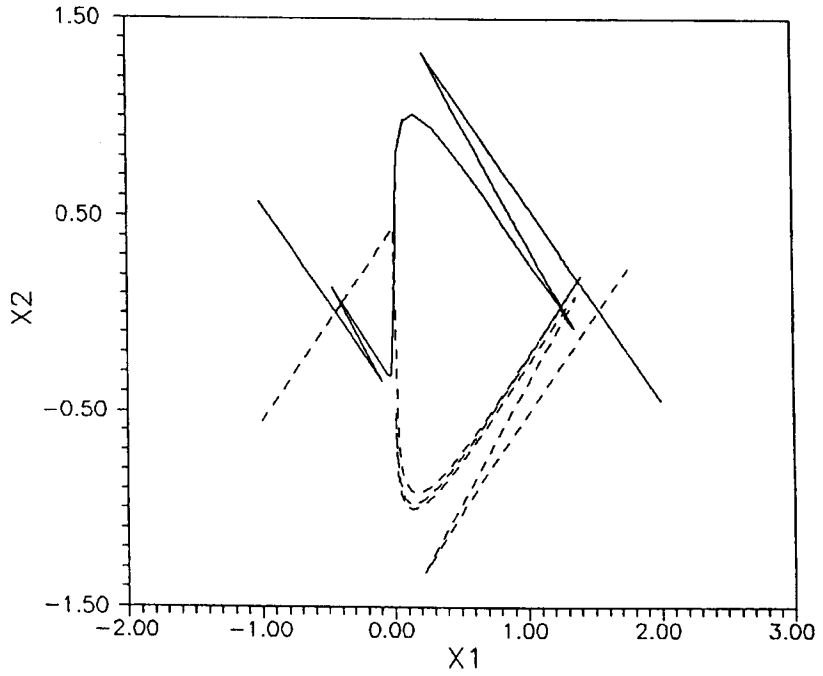

Figure 4. Stable (solid line) and unstable (dashed line) invariant manifolds on the Poincaré section, $(A, \Omega, e, \Phi) = (4.6, 2.7, 0.5, 3.14)$.

to be a unified measure for both perturbed and unperturbed chaotic responses. The Foguel alternative theorem is employed here to assert the existence of invariant measure (time-averaged PDF). Numerical results are interpreted in light of this theorem to infer asymptotic stabilities of responses.

For the purpose of this study, the Foguel alternative theorem may be stated as follow (for a more formal mathematical statement, see [25]):

A continuous stochastic Markov process governed by the Fokker–Planck equation possesses either an asymptotic stationary PDF or sweeping properties with respective to a particular region of interest containing the responses. If within the region of interest:

(a) the Markov process is periodic, i.e., there exists a time shift t_0 such that the PDFs corresponding to time t and $t + t_0$ are identical, then a stationary PDF (equivalently an invariant measure) exists and is equal to the averaged value of the PDFs over the (steady-state) period t_0. Therefore, when periodicity in the evolution of PDF is detected, an invariant measure is assured and the response of the system is asymptotically stable.

(b) the Markov process is aperiodic (i.e. a stationary density does not exist), then all probability mass (i.e. volume of PDF) will eventually escape (or be swept) out of the region and hence asymptotically unstable.

Numerical results consistent with the Foguel alternative theorem will be demonstrated in the following sections.

4. Chaotic and Overturning Response

The behavior of the rocking system is very rich in terms of diverse nonlinear responses [5–8]. Among them, the chaotic (long-term unpredictable) and the overturning (unbounded) responses are of most interest. In this section, relationships between these two critical rocking responses are examined in both deterministic and stochastic states.

4.1. Deterministic State

4.1.1. *Chaotic Response*

Chaotic response may occur in a deterministic state when the Melnikov criterion is satisfied. A sample chaotic response of the rocking system is shown in Figure 5. The unpredictability (sensitivity to initial conditions) of the chaotic response is demonstrated by the time histories shown in Figure 5a. It is observed that, with a small variation in the initial conditions, the rocking system will result in totally different chaotic response trajectories. Fractal properties of the chaotic attractor via the Poincaré map are shown in Figure 5b. Note that as indicated by the Melnikov criterion (equation (11)), the possible chaotic domain expands when e increases. On the other hand, the domain of stable rocking responses shrinks with increasing e [7]. Thus, these possible chaotic responses may occur in the transient prior to overturning. Extensive numerical studies shall be conducted to identify the existence of chaotic response with large values of e. In this study, for the purpose of demonstrating the invariant structure of steady-state chaos (Section 4.1.2), e is chosen 0.5 here together with large periodic excitation to assure steady-state chaotic rocking response.

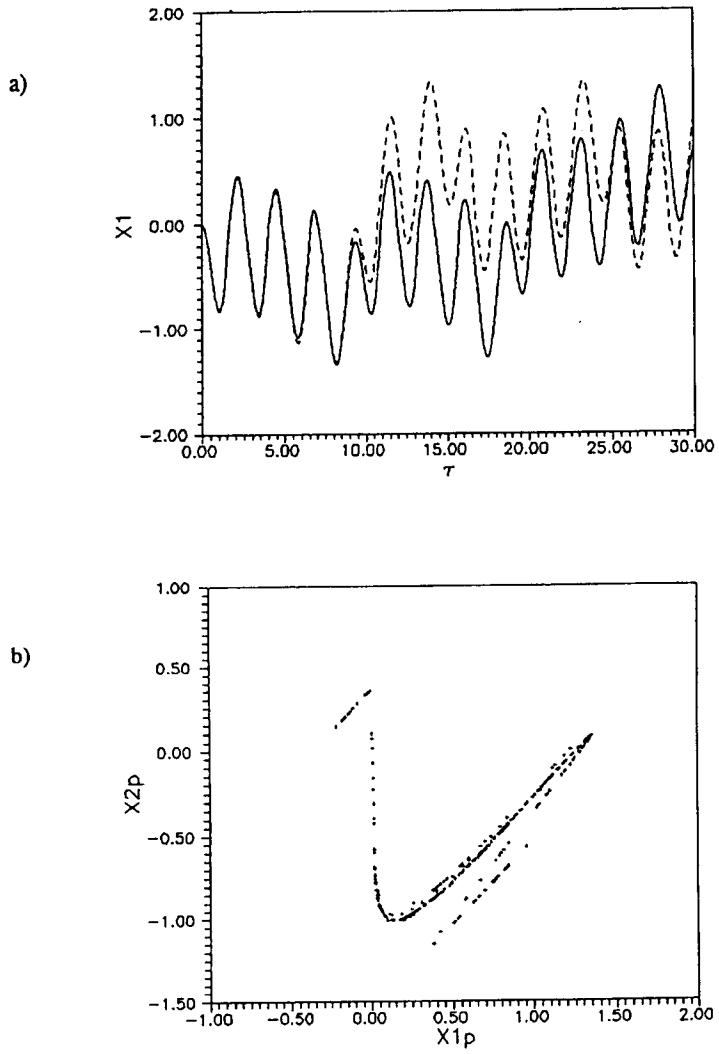

Figure 5. Deterministic chaotic rocking response: (a) sensitivity to initial conditions in time histories; (b) corresponding strange attractor in Poincaré map; $(A, \Omega, e, \Phi) = (4.6, 2.7, 0.5, 3.14)$.

4.1.2. *Stochastic Properties of Deterministic Chaotic Response*

An ensemble numerical experiment has been conducted to demonstrate the stochastic properties of the deterministic chaotic rocking response with uniformly distributed initial uncertainties [8]. In this study, 5000 realizations of chaotic response with initial conditions corresponding to grid points in a small square are generated and sampled after 500 cycles of the forcing period (T). Figure 6 shows the marginal PDF corresponding to a typical chaotic response sampled with various shifts, i.e., $\Psi = 0.0 \times T, 0.2 \times T, 0.4 \times T, 0.6 \times T, 0.8 \times T$ and $1.0 \times T$. It is shown that the PDFs are practically identical when the shift is at integer multiples of the forcing period, i.e., $0.0 \times T$ and $1.0 \times T$. The PDFs appear to be symmetric about the half-cycle time point, i.e., at $0.2 \times T$ and $0.8 \times T$, and at $0.4 \times T$ and $0.6 \times T$. Thus periodicity in the evolution is demonstrated. Based on part (a) of the Foguel alternative theo-

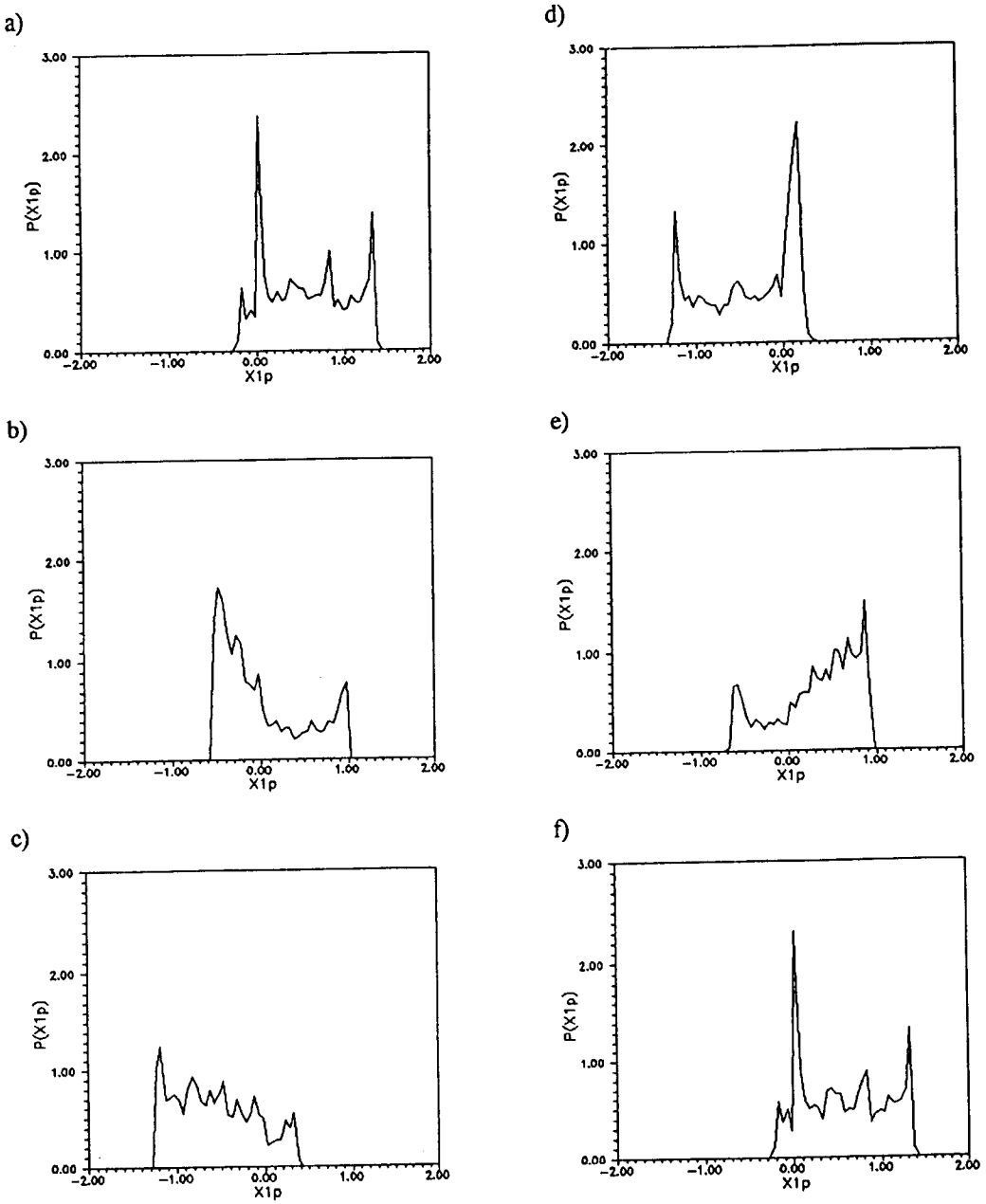

Figure 6. Periodicity in the evolution of PDF of chaotic rocking response: $\Psi =$ (a) $0.0 \times T$, (b) $0.2 \times T$, (c) $0.4 \times T$, (d) $0.6 \times T$, (e) $0.8 \times T$, and (f) $1.0 \times T$; $(A, \Omega, e, \Phi) = (4.6, 2.7, 0.5, 3.14)$.

rem, a stationary PDF (and hence an invariant measure) exists. For this example, the time shift t_0 is equal to excitation period, T. The corresponding time-averaged PDF (invariant measure) is shown in Figure 7. Thus the combination of numerical results and the Foguel alternative theorem assures that sample deterministic chaotic rocking responses in the attracting region are bounded and asymptotically stable.

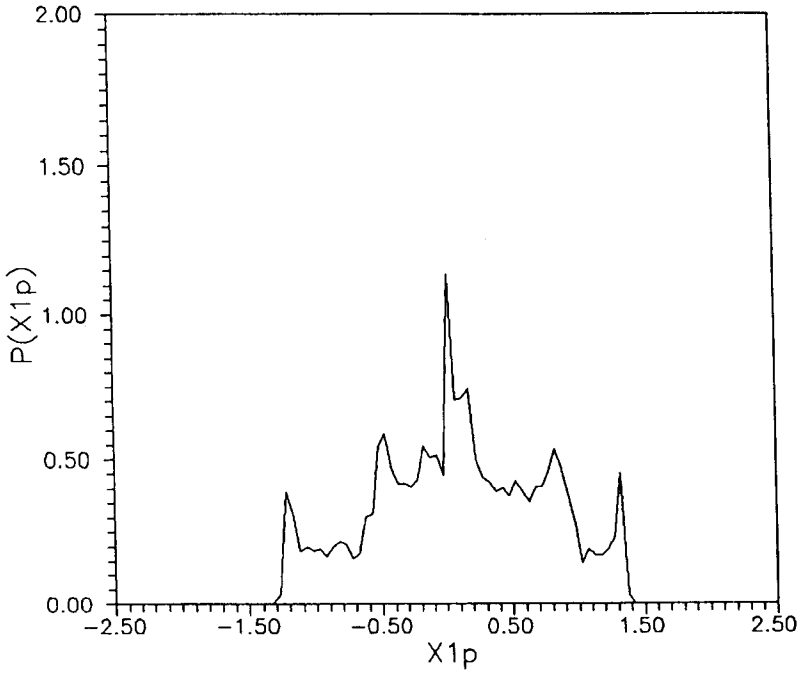

Figure 7. Time-averaged PDF (invariant measure) of chaotic rocking response; $(A, \Omega, e, \Phi) = (4.6, 2.7, 0.5, 3.14)$.

4.1.3. *Overturning Response*

Due to the heteroclinic nature of the rocking system, overturning response can easily result if the periodic excitation amplitude is sufficiently large or the initial value is in the "unsafe region". The region is deemed safe if initial conditions within which bounded rocking responses (periodic or chaotic) result. Similarly, the region is deemed unsafe if initial conditions within which unbounded rocking responses (overturning) occur. The boundary between safe and unsafe regions is simple (smooth) in a periodic state [26]. However, this boundary may be fractal when the system is chaotic. Identification of the boundary of the safe region in a chaotic state has to rely on an extensive numerical investigation [27]. Nevertheless, in a chaotic state, the tangled invariant manifolds qualitatively indicate the boundary of the domain of attraction. Thus the region enclosed by the invariant manifolds may yield the defining area for further numerical search to identify the fractal details of the boundary for the safe region.

Figure 8a indicates the possible safe regions for the unperturbed/Hamiltonian system (enclosed by the dashed line) and the perturbed, damped and forced system (enclosed by the solid line). It is observed that the possible safe region has been shifted to the right due to the presence of the external perturbations (periodic excitation). Figure 8b shows a bounded chaotic time history with initial conditions $(0.90, 0.36)$ which is located inside the perturbed safe region but outside the unperturbed safe region. Figure 8c shows an overturning rocking response with initial conditions $(-0.8, 0.0)$ which is located inside the unperturbed safe region but outside the perturbed safe region. These numerical observations confirm that when the rocking system is perturbed (forced), the invariant manifolds provide the imprint of the safe region.

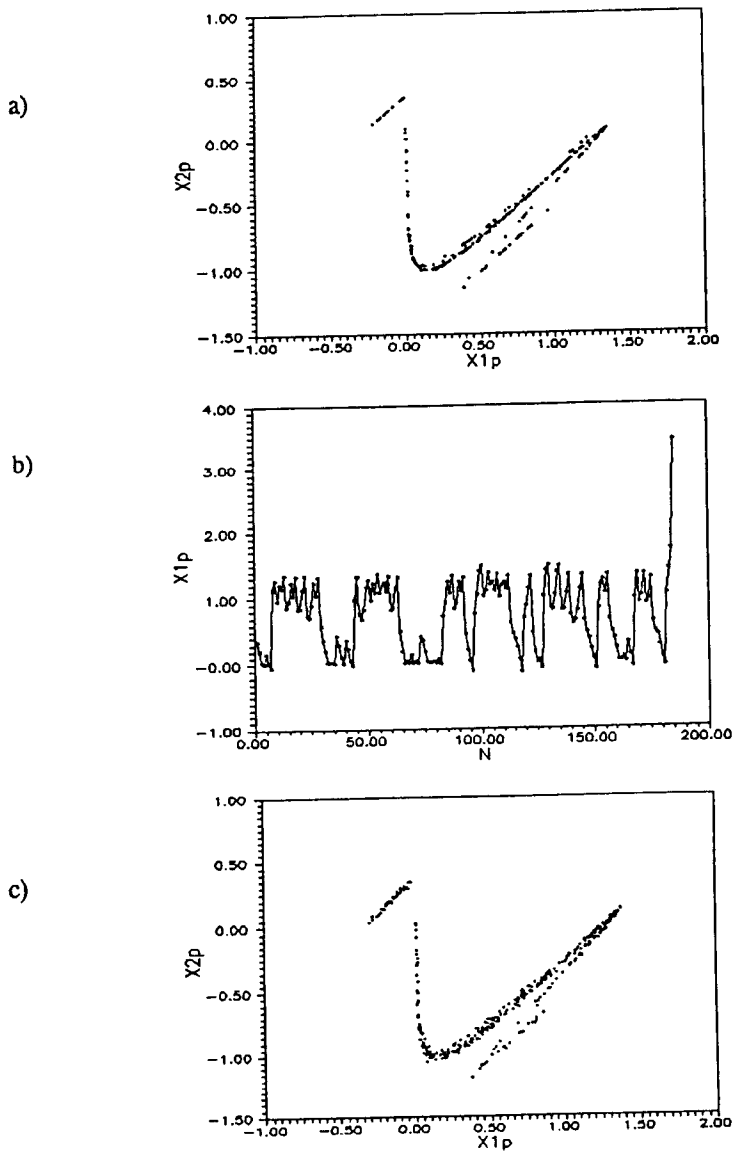

Figure 10. Sensitivity of chaotic response to noise perturbations and corresponding mean Poincaré map: (a) deterministic ($\sigma^2 = 0.0$); (b) weak noise leads to overturning ($\sigma^2 = 0.04^2$, Poincaré points vs. Nth forcing period); (c) mean Poincaré map corresponding to (b); $(A, \Omega, e, \Phi) = (4.6, 2.7, 0.5, 3.14)$.

chaos). Moreover, if a response is chaotic in the deterministic state (Figure 10a), it could be brought out of the chaotic state and led to overturning due to the presence of external noise (Figure 10b). These numerical results indicate that the presence of additive noise expedites the occurrence of chaotic rocking and overturning responses in parameter space and reduces the stability of the response behavior.

4.2.2. *Overturning Response*

The PDFs obtained through the Markov process approximation can supply global information about rocking response behavior. The external random noise plays a role of bridging all coexisting attracting domains. The corresponding PDFs portray these attractors on a Poincaré map and indicate their relative strengths.

Figure 11 shows the evolution of the PDFs in the first few cycles of excitation period. Starting with quiescent initial condition $(0, 0)$, the PDF is concentrated in the safe region for the first two cycles (Figures 11a and b), and then spreads widely over phase space after two and a half cycles (Figure 11c). This indicates that the domains of attractions of all coexisting attractors are bridged by the external noise. Continuing integration of the PDF (not shown here) shows that spreading of the PDF continues with increasing number of excitation cycles and eventually all probability mass is swept out of the region of interest (in this case region bounded by $\pm\pi/2\theta_{cr}$ normalized angular displacements). This result implies that the overturning region (diverging to $\pm\infty$ displacements) is a much stronger attractor compared to the other coexisting attracting domains of bounded responses (periodic and chaotic). These numerical results are consistent with part (b) (sweeping property) of the Foguel alternative. Because a stationary density (invariant measure) does not exists within the region of interest, all probability mass will eventually escape (be swept) from the region. Sweeping of the probability mass from the stable (non-overturning) region indicates that the rocking system is asymptotically unstable with the presence of white noise, thus all perturbed response trajectories will eventually diverge to overturning (or, in other words, converge to the overturning attractors).

As mentioned previously, although the ideal white noise is not realized in practice because of its infinite variance, results from the Markov process (which is based on white-noise assumption) do indicate the intrinsic characteristics of the rocking response behavior. A limited parametric simulation study has been conducted, and numerical results of randomly disturbed chaotic responses based on finite-variance Shinozuka's noise do escape out of the bounded domain into the overturning domain within finite duration. An example of a chaotic response under relatively weak Shinozuka's noise perturbations ($\sigma^2 = 0.04^2$) is shown in Figure 10b. Compared to the overturning attractor, the weak stability of the chaotic attractor is indicated by the corresponding PDF obtained from the Markov process approximation, as shown in Figure 11.

4.2.3. *Reconstruction of Chaotic Attractor*

As demonstrated in a previous section, numerical results indicate that all bounded motions are weakly stable compared to overturning. Due to the overwhelming strength of the overturning attractor and the noise-induced bridging effect on domains of attraction of coexisting attractors, after a sufficient long but finite duration, all bounded motions will eventually escape to the overturning region. In reality, except when under very strict control, noise perturbations in a rocking system are inevitable. Thus, the strange attractor embedded in the stochastic state and the associated transient chaotic rocking response may be difficult to detect due to the strong attraction of overturning. However, through the mean Poincaré map, the fractal structure of the corresponding embedded chaotic attractor can be reconstructed. Figure 10b shows a chaotic time history which leads to overturning due to the presence of noise perturbations, i.e., transient chaos (also see Figure 9b). Figure 10c illustrates that when the noise perturbations are averaged out through the mean Poincaré mapping technique, the embedded chaotic attractor

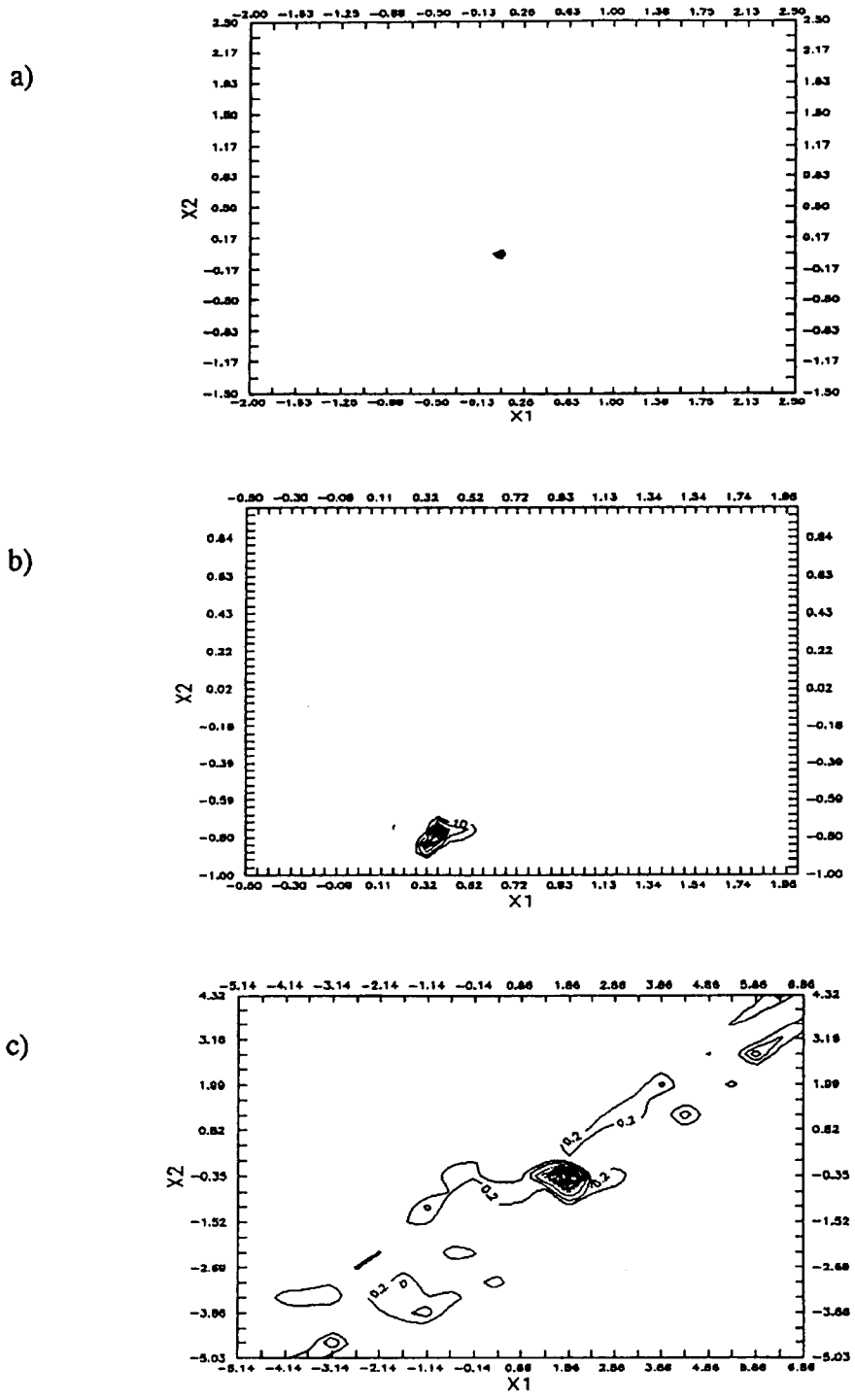

Figure 11. Evolution of PDF: (a) initial probability concentrated at (0.0, 0.0); (b) PDF after one cycle of the forcing period; (c) PDF after 2.5 cycles of the forcing period (overturning occurs), $(A, \Omega, e, \kappa, \Phi) = (4.6, 2.7, 0.5, 0.003, 3.14)$.

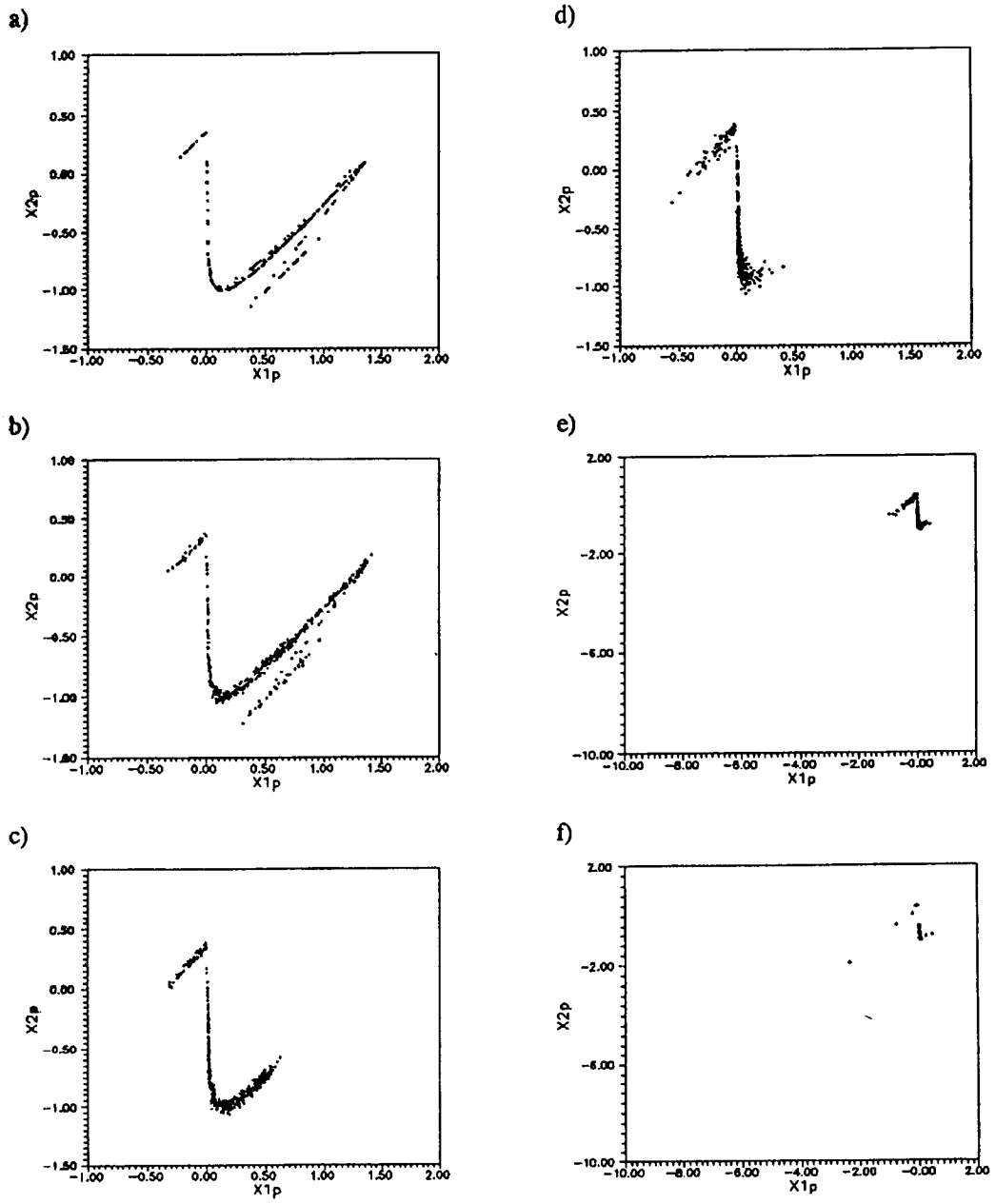

Figure 12. Capability of mean Poincaré map at various noise levels: (a) $\sigma^2 = 0.0$, (b) $\sigma^2 = 0.05^2$, (c) $\sigma^2 = 0.06^2$, (d) $\sigma^2 = 0.12^2$, (e) $\sigma^2 = 0.13^2$, and (f) $\sigma = 0.16^2$, $(A, \Omega, e, \Phi) = (4.6, 2.7, 0.5, 3.14)$.

surfaces on the Poincaré section. The fractal details in the reconstructed strange attractor implying "orderness" in the corresponding chaotic response are not destroyed by the presence of noise. Thus transient chaos may be exhibited with noise present (Figures 9b and 10b).

The capability of the mean Poincaré map to reconstruct chaotic attractors via various noise intensities is further demonstrated in Figure 12. Compared to the chaotic attractor in the

deterministic state (Figure 12a), the mean Poincaré map preserves the fractal characteristics with a low level noise perturbations ($\sigma^2 \leq 0.05^2$, Figure 12b). When the noise intensity increases ($0.06^2 \leq \sigma^2 \leq 0.12^2$), although the mean Poincaré points are still in the bounded region (Figures 12c and d), the fractal structure of the embedded chaotic attractor deteriorates, which indicates that the "orderness" of the chaotic response in the stochastic state is diminished by the noise. When the noise intensity further increases ($\sigma^2 \geq 0.13^2$), overturning response results in the mean sense (Figures 12e and f).

Numerical results here indicate that when the noise level is low ($\sigma^2 \leq 0.05^2$), most of the deterministic features of perturbed rocking responses are preserved, and the corresponding embedded attractor can be reconstructed. The block may experience transient chaos with low-intensity noise prior to eventual overturning. When the noise level is high ($0.06^2 \leq \sigma^2 \leq 0.12^2$) the noise-induced randomness prevails the "orderness" of the response, and a random-like cluster is shown in the mean Poincaré map. Thus, the block rocks essentially in a random fashion. Similar noise-induced "orderness" elimination has also been observed in the literature via the smoothing of marginal PDF and Lyapunov exponent [28, 29]. When the noise level further elevates ($\sigma^2 \geq 0.13^2$), the block overturns with practical certainty in the mean sense.

5. Concluding Remarks

The rocking behavior of a slender rigid object subjected to periodic excitation with and without noise perturbations has been examined to gain a better understanding of its sensitivity and stability. The close relationship between chaotic and overturning responses in the vicinity of the heteroclinic orbits has been demonstrated in both deterministic and stochastic states. The following concluding remarks are expressed:

1. A generalized stochastic Melnikov process have been derived by taking into account the presence of random noise. The resulting criterion can provide a lower bound for possible chaotic domain in parameter space. Numerical results show that the presence of random noise expedites the occurrence of possible chaotic and overturning responses of the rocking system and decreases the stability of the response behavior in general.
2. The Markov process approximation provides global information about rocking response behaviors and their relative strengths. A fast diverging PDF of the perturbed chaotic rocking response indicates its asymptotical instability with noise present.
3. In the deterministic chaotic state, the tangled invariant manifolds provide an imprint of the boundary for the safe region in phase space and demonstrate the close relationship between the chaotic and overturning responses in terms of domain of attraction.
4. Domains of attraction of all coexisting responses may be bridged with the presence of random noise, thus the system may behave in a fashion of combined response characteristics. Numerical results indicate that among coexisting responses, the overturning attractor is of the greatest strength such that the block is led to overturn even when low-intensity random noise is present.
5. Identification of transient chaos and reconstruction of the corresponding embedded chaotic attractor in a noisy environment are accomplished by applying the mean Poincaré map. When random noise is present and the fractal details of the reconstructed strange attractor are preserved in the mean Poincaré map, the rigid object may experience transient chaotic rocking response prior to eventual overturning.
6. The Foguel alternative theorem is numerically demonstrated in the perturbed/unperturbed rocking system. When the rocking system is in a deterministic state, the deterministic

chaotic response is asymptotically stable and an invariant measure (time-averaged PDF) exists. When the rocking system is in a stochastic state (with white noise present), sweeping of the PDF from the stable region indicates the system is asymptotically unstable.

Acknowledgements

The authors gratefully acknowledge the financial support from the United States Office of Naval Research (Grant No. N00014-92-J-1221).

References

1. Aslam, M., Godden, W. G., and Scalise, D. T., 'Earthquake rocking response of rigid bodies', *Journal of Structural Engineering Division, ASCE* **106**, 1980, 377–392.
2. Yim, S. C. S., Chopra, A. K., and Penzien, J., 'Rocking response of rigid blocks to earthquakes', *Earthquake Engineering and Structural Dynamics* **8**, 1980, 565–587.
3. Spanos, P. D. and Koh, A. S., 'Rocking of rigid blocks due to harmonic shaking', *Journal of Engineering Mechanics Division, ASCE* **110**, 1984, 1627–1642.
4. Wong, C. M. and Tso, W. K., 'Steady state rocking response of rigid blocks, Part II: Experiment', *Earthquake Engineering and Structural Dynamics* **18**, 1989, 107–120.
5. Hogan, S. J., 'On the dynamics of rigid-block motion under harmonic forcing', *Proceedings of Royal Society of London A* **425**, 1989, 441–476.
6. Yim, S. C. S. and Lin, H., 'Nonlinear impact and chaotic response of slender rocking objects', *Journal of Engineering Mechanics Division, ASCE* **117**, 1991, 2079–2100.
7. Yim, S. C. S. and Lin, H., 'Chaotic behavior and stability of free-standing offshore equipment', *Ocean Engineering* **18**, 1991, 225–250.
8. Yim, S. C. S. and Lin, H., 'Probabilistic analysis of a chaotic dynamical system', in *Applied Chaos*, J. H. Kim and J. Stringer (eds.), John Wiley & Sons, New York, 1992, pp. 219–241.
9. Koh, A. S., 'Rocking of rigid blocks on randomly shaking foundations', *Nuclear Engineering and Design* **97**, 1986, 269–276.
10. Iyengar, R. N. and Manohar, C. S., 'Rocking response of rectangular rigid blocks under random noise base excitations', *International Journal of Non-Linear Mechanics* **26**, 1991, 885–892.
11. Dimentberg, M. F., Lin, Y. K., and Zhang, R., 'Toppling of computer-type equipment under base excitation', *Journal of Engineering Mechanics Division, ASCE* **119**, 1993, 145–160.
12. Bruhn, B. and Koch, B. P., 'Heteroclinic bifurcations and invariant manifolds in rocking block dynamics', *Zeitschrift für Naturforschung* **46a**, 1991, 481–490.
13. Lin, H. and Yim, S. C. S., 'Nonlinear rocking motions, II: Overturning under random excitations', to appear in *Journal of Engineering Mechanics Division, ASCE*.
14. Kapitaniak, T., *Chaos in Systems with Noise*, World Scientific, Singapore, 1988.
15. Risken, H., *The Fokker–Planck Equation: Methods of Solution and Applications*, Springer-Verlag, Berlin/Heidelberg, 1984.
16. Wu, Y. J., Yim, S. C. S., and Lin, H., 'Stochastic response of chaotic systems to combined periodic and random excitations', Report No. OE-95-05, Oregon State University, Ocean Engineering Program, 1995.
17. Guckenheimer, J. and Holmes P., *Nonlinear Oscillations, Dynamical Systems, and Bifurcations of Vector Fields*, Springer-Verlag, New York, 1983.
18. Wiggins, S., *Introduction to Applied Nonlinear Dynamical Systems and Chaos*, Springer-Verlag, New York, 1990.
19. Jordan, D. W. and Smith, P., *Nonlinear Ordinary Differential Equations*, Oxford University Press, Oxford, 1987.
20. Parker, T. S. and Chua, L. O., *Practical Numerical Algorithms for Chaotic Systems*, Springer-Verlag, New York, 1989.
21. Haken, H., 'Generalized Onsager–Machlup function and classes of path integral solutions of the Fokker–Planck equation and the Master equations', *Zeitschrift für Physik B* **24**, 1976, 321–326.
22. Wehner, M. F. and Wolfer, W. G ., 'Numerical evaluation of path-integral solutions to Fokker–Planck equations', *Physical Review A* **27**, 1983, 2663–2670.
23. Shinozuka, M., 'Simulation of multivariate and multidimensional random processes', *Journal of Acoustical Society of America* **49**, 1977, 357–367.
24. Thompson, J. M. T. and Stewart, H. B., *Nonlinear Dynamics and Chaos*, John Wiley & Sons, Chichester, 1986.

25. Lasota, A. and Mackey, M. C., *Chaos, Fractals, and Noise*, 2nd Ed., Springer-Verlag, New York, 1994.
26. Falzarano, J., Shaw, S. W., and Troesch, A. W., 'Application of global methods for analyzing dynamical systems to ship rolling motion and capsizing', *International Journal of Bifurcation and Chaos* **2**, 1992, 101–115.
27. Thompson, J. M. T., Bishop, S. R., and Leung, L. M., 'Fractal basins and chaotic bifurcations prior to escape from a potential well', *Physics Letters A* **121**, 1987, 116–120.
28. Bulsara, A. R. and Jacobs, E. W., 'Noise effects in a nonlinear dynamic system: the rf superconducting quantum interference device,' *Physical Review A* **42**, 1990, 4614–4621.
29. Crutchfield, J. P., Farmer, J. D., and Huberman, B. A., 'Fluctuations and simple chaotic dynamics', *Physics Reports* **92**, 1982, 45–82.